

# Coupling of T161 and T14 phosphorylations protects cyclin B–CDK1 from premature activation

Katia Coulonval<sup>a</sup>, Hugues Kooken<sup>a</sup>, and Pierre P. Roger<sup>a,b</sup>

<sup>a</sup>Institute of Interdisciplinary Research (IRIBHM), Université Libre de Bruxelles, Campus Erasme, B-1070 Brussels, Belgium; <sup>b</sup>WELBIO

**ABSTRACT** Mitosis is triggered by the abrupt dephosphorylation of inhibitory Y15 and T14 residues of cyclin B1-bound cyclin-dependent kinase (CDK1) that is also phosphorylated at T161 in its activation loop. The sequence of events leading to the accumulation of fully phosphorylated cyclin B1–CDK1 complexes remains unclear. Two-dimensional gel electrophoresis allowed us to determine whether T14, Y15, and T161 phosphorylations occur on same CDK1 molecules and to characterize the physiological occurrence of their seven phosphorylation combinations. Intriguingly, in cyclin B1–CDK1, the activating T161 phosphorylation never occurred without the T14 phosphorylation. This strict association could not be uncoupled by a substantial reduction of T14 phosphorylation in response to Myt1 knockdown, suggesting some causal relationship. However, T14 phosphorylation was not directly required for T161 phosphorylation, because Myt1 knockdown did uncouple these phosphorylations when leptomycin B prevented cyclin B1–CDK1 complexes from accumulating in cytoplasm. The coupling mechanism therefore depended on unperturbed cyclin B1–CDK1 traffic. The unexpected observation that the activating phosphorylation of cyclin B1–CDK1 was tightly coupled to its T14 phosphorylation, but not Y15 phosphorylation, suggests a mechanism that prevents premature activation by constitutively active CDK-activating kinase. This explained the opposite effects of reduced expression of Myt1 and Wee1, with only the latter inducing catastrophic mitoses.

**Monitoring Editor**  
Mark J. Solomon  
Yale University

Received: Feb 15, 2011  
Revised: Aug 19, 2011  
Accepted: Sep 1, 2011

## INTRODUCTION

The major events of the eukaryotic cell cycle depend on the sequential formation, activation (by phosphorylation and/or dephosphorylation), and then inactivation of different complexes of cyclin-dependent kinases (CDKs). In animal cells, the activation of cyclin B1–CDK1 triggers the abrupt transition from interphase to mitosis, depending

on correct termination of genome duplication (reviewed in Nigg [2001] and Lindqvist *et al.* [2009]). Moreover, CDK1 is the only required cell cycle CDK for the first part of development in mice (Santamaria *et al.*, 2007). It can replace CDK2 in S-phase control (Berthet and Kaldis, 2006; Hochegger *et al.*, 2007; Santamaria *et al.*, 2007), and cyclin A2-CDK1 has been found to regulate the firing of late DNA replication origins (Katsuno *et al.*, 2009). On the other hand, roles of cyclin A2-CDK2 (Guadagno and Newport, 1996; Furuno *et al.*, 1999) and cyclin A2-CDK1 in mitosis and priming cyclin B1–CDK1 activation have been partially clarified recently (Fung *et al.*, 2007; Gong *et al.*, 2007; De Boer *et al.*, 2008; Deibler and Kirschner, 2010; Gong and Ferrell, 2010).

The mechanisms by which the activity of cyclin B1–CDK1 is regulated spatially and temporally have been intensely investigated for two decades. Cyclin A2 and cyclin B1 accumulate during S and G2 phases and are degraded during mitosis. Whereas cyclin A2 is nuclear, cyclin B1–CDK1 complexes are mostly cytoplasmic during interphase (Pines and Hunter, 1991; Bailly *et al.*, 1992). They are first activated on centrosomes (Jackman *et al.*, 2003; Kramer *et al.*,

This article was published online ahead of print in MBoC in Press (<http://www.molbiolcell.org/cgi/doi/10.1091/mbc.E11-02-0136>) on September 7, 2011.

The authors declare they have no conflict of interest.

Address correspondence to: Pierre P. Roger ([proger@ulb.ac.be](mailto:proger@ulb.ac.be)).

Abbreviations used: BrdU, bromodeoxyuridine; CAK, CDK-activating kinase; CDK, cyclin-dependent kinase; EdU, 5-ethynyl-2'-deoxyuridine; EGTA, ethylene glycol tetraacetic acid; ER, endoplasmic reticulum; FBS, fetal bovine serum; LMB, leptomycin B; N+G, nuclear plus Golgi; PBS, phosphate-buffered saline; PVDF, polyvinylidene fluoride; siRNA, small interfering RNA.

© 2011 Coulonval *et al.* This article is distributed by The American Society for Cell Biology under license from the author(s). Two months after publication it is available to the public under an Attribution–Noncommercial–Share Alike 3.0 Unported Creative Commons License (<http://creativecommons.org/licenses/by-nc-sa/3.0>).

“ASCB®,” “The American Society for Cell Biology®,” and “Molecular Biology of the Cell®” are registered trademarks of The American Society of Cell Biology.

2004), and their subsequent nuclear import just before nuclear envelope breakdown coincides with a dramatic activation of the whole pool of cyclin B1–CDK1 complexes, leading to triggering of mitosis (Gavet and Pines, 2010a, 2010b). In addition to cyclin binding, CDK1 activity requires the phosphorylation at T161 of its activation segment (Krek and Nigg, 1992; Solomon *et al.*, 1992) by the nuclear CDK-activating kinase (CAK), constituted by the cyclin H-CDK7 complex, which is constitutively active during cell cycle and thus not a likely target of regulatory mechanisms (Darbon *et al.*, 1994; Fisher and Morgan, 1994; Solomon, 1994; Tassan *et al.*, 1994; Larochelle *et al.*, 2007). During interphase, the activity of CDK1 is restricted by inhibitory phosphorylations in the active site on Y15 and to a lesser extent on T14 (Krek and Nigg, 1991a; Norbury *et al.*, 1991), respectively performed in human cells by Wee1 (Parker and Piwnicka-Worms, 1992; Parker *et al.*, 1995; Watanabe *et al.*, 1995) and Myt1 (Booher *et al.*, 1997; Liu *et al.*, 1997). Cyclin B1–CDK1 activation and mitosis firing depend on the abrupt dephosphorylation of these residues by Cdc25 phosphatases when their activity exceeds that of Wee1 and Myt1 kinases (reviewed in Nilsson and Hoffmann [2000]). This process ensures the dependence of mitosis upon correct termination of DNA replication and is halted by DNA damage, which is mediated by inhibition of Cdc25 phosphatases by the checkpoint kinases Chk1 and Chk2 (Mailand *et al.*, 2002; Sorensen *et al.*, 2003; Kramer *et al.*, 2004; Schmitt *et al.*, 2006). Accordingly, vertebrate cells overexpressing CDK1 with T14A and Y15F substitutions (CDK1AF; Krek and Nigg, 1991b; Norbury *et al.*, 1991; Potapova *et al.*, 2009) or treated with Wee1 small interfering RNAs (siRNAs; Nakajima *et al.*, 2008) undergo mitotic catastrophe (*i.e.*, entry into mitosis before completion of DNA replication, resulting in aberrant mitosis and cell death). Various positive and double negative feedback loops involving activation of Cdc25 phosphatases and inhibition of Wee1 and Myt1 by CDK1 and other kinases, such as Plk1, ensure the bistable, switch-like, character of cyclin B1–CDK1 activation and its hypersensitivity to cyclin B1 accumulation (Pomerening *et al.*, 2003; Lindqvist *et al.*, 2009; Deibler and Kirschner, 2010).

This model implies that the trigger of cyclin B1–CDK1 activation and mitosis is the dephosphorylation of Y15 and T14 residues, rather than T161 phosphorylation. To avoid premature (catastrophic) mitosis, activating and inhibitory phosphorylations of CDK1 should either coincide or inhibitory phosphorylations should precede the activating phosphorylation. Whether one of these possibilities indeed occurs in the cell has not been observed directly, because a technique that allows one to associate the different phosphorylations in one single CDK1 molecule has never been used consistently. The three phosphorylations of CDK1 depend on its binding to a cyclin (Solomon *et al.*, 1990, 1992; Meijer *et al.*, 1991; Parker *et al.*, 1991; Liu *et al.*, 1997; Larochelle *et al.*, 2007), but the stable association of cyclin B1 and CDK1 itself depends on its activating T161 phosphorylation (Larochelle *et al.*, 2007). How the different phosphorylations could be coordinated is also unclear, if one considers the different subcellular compartmentalizations, before mitosis, of cyclin B1–CDK1 complex (mostly cytoplasmic; Pines and Hunter, 1991; Bailly *et al.*, 1992), CAK (nuclear; Tassan *et al.*, 1994), Wee1 (nuclear; Heald *et al.*, 1993; Baldin and Ducommun, 1995), and Myt1 (associated to endoplasmic reticulum [ER] and Golgi membranes; Kornbluth *et al.*, 1994; Booher *et al.*, 1997; Liu *et al.*, 1997).

We have previously shown that the high-resolution power of two-dimensional gel electrophoresis, coupled to detection using phosphospecific antibodies, allows one to visualize the various (multi-)phosphorylated forms of endogenously expressed CDK2, CDK4, and CDK6 associated with their regulatory partners, which permitted us to make novel observations (Bockstaele *et al.*, 2006,

2009; Coulonval *et al.*, 2003a, 2003b). In this study, we applied this approach to reassess in two human cell models of cell cycle progression the precise relationship between the different phosphorylations of CDK1, its binding to cyclins, and its compartmentalization.

## RESULTS

Two human cell cycle models were used: the synchronous progression in S, G2, and M phases of HeLa cells after release from a double thymidine block (Figure 1A) and the massive and relatively synchronous cell cycle entry and progression induced by serum stimulation of quiescent T98G cells (Figure 1B). Synchrony of the cultures was monitored by bromodeoxyuridine (BrdU) incorporation and detection of phosphohistone H3. Eighty to ninety percent of cells were observed in S phase until 7 h after thymidine removal in HeLa cells and 16–20 h after serum stimulation in T98G cells. Mitoses mostly appeared ~10 h after release in HeLa cells and 24–26 h after stimulation of T98G cells (Figure 1, A and B, respectively). In SDS–PAGE, CDK1 separated into three bands (1, 2, 3), band 1 being the most abundant. As confirmed using phosphospecific antibodies to CDK1 (which also recognize phosphorylated CDK2 [Figure 1, asterisk]), band 2 reflected inhibitory phosphorylations on either T14 or Y15, and their combination generated band 3, whereas the activating T161 phosphorylation did not affect CDK1 migration and is therefore observed in all three bands (Krek and Nigg, 1991a; Norbury *et al.*, 1991; Solomon *et al.*, 1992; Atherton-Fessler *et al.*, 1994). Consistent with previous characterizations, all three phosphorylations increased as cells progressed in S to M phase, in parallel with the accumulation of cyclin A2 and cyclin B1. T161 phosphorylation was mainly associated with T14 and Y15 phosphorylations in band 3 but appeared in the lower band 1 when mitoses were detected.

In T98G cells, Wee1 and Myt1 were induced 6 and 10 h, respectively, after serum addition and accumulated maximally during S phase. In both T98G and HeLa cells, they displayed complex profiles, with upper bands increasing during S and G2 phases (Figure 1, A and B), likely due to various phosphorylations, including those by cyclin A/B-CDK (Watanabe *et al.*, 1995; Booher *et al.*, 1997; Liu *et al.*, 1997; Deibler and Kirschner, 2010). A sudden additional mobility shift of Myt1 was observed in mitotic cells, corresponding to its inactivated multiphosphorylated forms.

### Two-dimensional gel separation of CDK1 phosphorylated forms

To simultaneously visualize all the different phosphorylated forms of CDK1, denatured lysates of synchronized HeLa cells in G2 and M phase were mixed, and CDK1 was immunoprecipitated using the C-19 CDK1 polyclonal antibody. Proteins were separated by IEF (pH 3–10 linear gradient), which was followed by SDS–PAGE and blotting. CDK1 and its phosphorylated forms were detected using mixtures of one phosphospecific CDK1 antibody (T14, T161, or Y15) and the A17 CDK1 monoclonal antibody and were revealed using mixed secondary antibodies coupled to DyLight 680 and 800 for two-color infrared fluorescence detection (Figure 2). CDK1 forms were distributed within an interval of 2.3 pH units. The most basic and abundant form of CDK1 (form 0) focused at approximately pH 8.5, close to the computed isoelectric point of human CDK1 (8.38). Besides CDK1 form 0 (and a slightly more basic minor satellite spot likely resulting from a covalent modification during sample preparation) and a second CDK1 form (form a), all the other forms of CDK1 were phosphorylated at Y15, T14, and/or T161, as detected by the phosphospecific antibodies (Figure 2). These different CDK1 phosphoforms and form a focused at positions that correspond to additions to CDK1 of entire numbers of negative charges

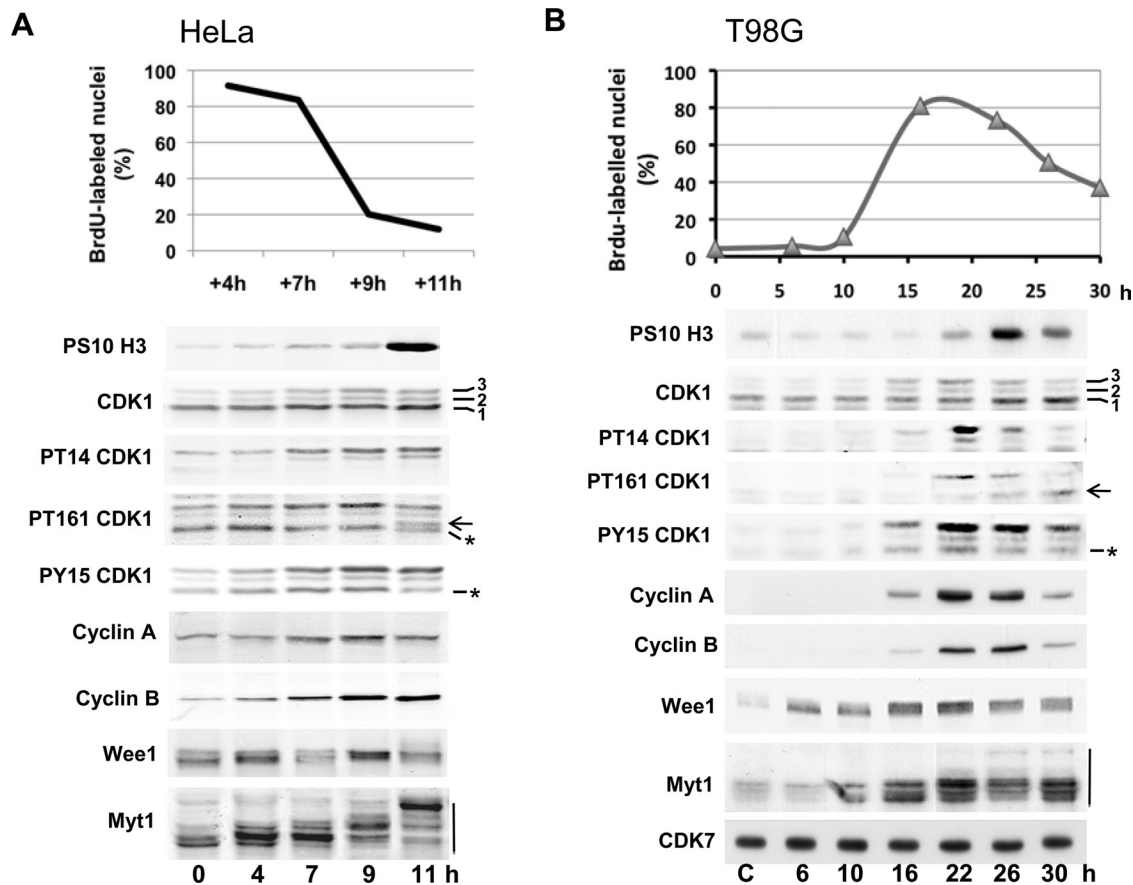


**FIGURE 1:** CDK1 and CDK1 regulatory proteins in synchronized HeLa and T98G cells. (A) HeLa cells were synchronized in G1/S by a double thymidine block. (B) Starved T98G cells (C, control) were reactivated by addition of 15% FBS. Synchrony of the cultures was monitored by counting the fraction of nuclei (mean of duplicate dishes) that incorporated BrdU during the last 30 min of the release/stimulation. Western blotting analysis was performed with the indicated antibodies from whole-cell extracts. In SDS-PAGE, CDK1 was separated in three bands (1, 2, 3). Arrows indicate the active single T161 phosphorylated form of CDK1 comigrating with band 1; asterisks identify CDK2 phosphorylated on T160 or Y15; mobility shift of Myt1 is indicated by a vertical line.

(position scale at the bottom of Figure 2B, computed according to Sillero and Ribeiro [1989] and Bjellqvist *et al.* [1993]). They were numbered according to their predicted number of phosphorylations relative to this scale (considering that phosphate groups produce a two-charge isoelectric point shift above pH 7 [ $\text{PO}_4^{2-}$ ] or a one-charge shift below this pH [ $\text{HPO}_4^-$ ]; Sillero and Ribeiro, 1989; Gianazza, 1995) and further labeled by their demonstrated phosphorylation(s), as illustrated in Figure 2B. The seven phosphorylated forms of CDK1 were thus resolved, including CDK1 phosphorylated at Y15 (1P15), T14 (1P14), T161 (1P161), the three twice-phosphorylated CDK1 forms (2P14,15; 2P14,161; 2P15,161), and CDK1 phosphorylated at the three residues (3P14,15,161). This determination is in perfect agreement with initial demonstrations by  $^{32}\text{P}$  incorporation and tryptic peptide and mutagenesis analyses, which did not detect any other important CDK1 phosphorylations in mammalian cells (Krek and Nigg, 1991a, 1992; Norbury *et al.*, 1991; Solomon *et al.*, 1992). CDK1 form a might be acetylated (Choudhary *et al.*, 2009), which neutralizes the positive charge of a lysine residue. This form was more consistently preserved by denaturing lysis and was never observed in cyclin-CDK1 complexes.

The phosphorylation pattern of total CDK1 was investigated during synchronous cell cycle progression in HeLa cells (Figure 3A). In S and G2 phases, 1P15; 2P14,15; and 3P14,15,161 were the most abundant phosphoforms. A minor proportion of 1P14 form was also

detected, as found in chicken CDK1 (Krek and Nigg, 1991a) but not observed in mouse CDK1 (Norbury *et al.*, 1991). The active 1P161 form was detected in S phase but was almost absent in G2 phase (Figure 3A). In G2 phase, T161 phosphorylation was associated with inhibitory phosphorylations (mostly at T14 and T14 + Y15). By contrast, in mitosis, 1P161 was the most abundant phosphorylated CDK1 form, and all the other phosphoforms were reduced. Identical observations were obtained in T98G cells (see Figures 4 and 5B). These observations support the notion that CDK1 activation in mitosis does not result from direct T161 phosphorylation of unphosphorylated CDK1, but from dephosphorylation of inhibitory residues, thus releasing the active CDK1 phosphorylated only at T161.

#### Only phosphorylation at T161, but not phosphorylation at Y15 and T14, is restricted to cyclin-bound CDK1

In HeLa cells (Figure 3B) and T98G cells (Figure 4), phosphorylation patterns were compared in CDK1 coimmunoprecipitated by cyclin B1 or cyclin A2 antibodies and in monomeric (free) CDK1. In HeLa cells, free CDK1 was obtained by immunoprecipitation with the C-19 CDK1 antibody after immunodepletion by cyclin antibodies. In T98G cells, free CDK1 was immunoprecipitated by the A17 monoclonal antibody, which does not precipitate CDK1 complexed to cyclins (Supplemental Figure S1C; Watanabe *et al.*, 1995). Phosphospecific CDK1 antibodies also detected phosphorylated

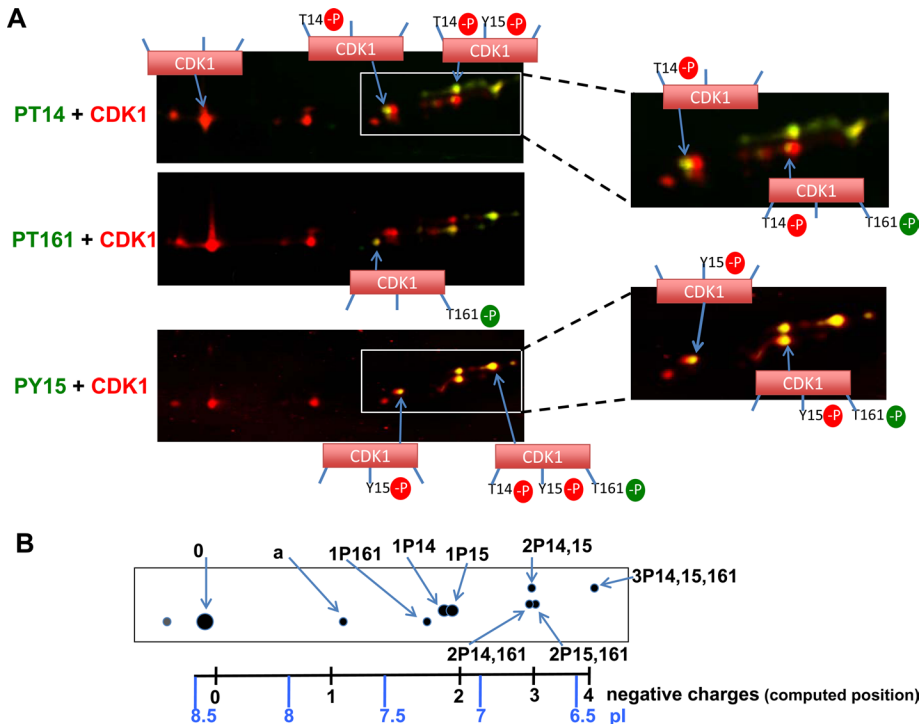


**FIGURE 2:** Identification of the multiple forms of CDK1 separated by two-dimensional gel electrophoresis. (A) Double immunofluorescence analysis of the two-dimensional gel electrophoresis pattern of total CDK1 immunoprecipitated from mixed samples of synchronized HeLa cells in G2 and mitosis. CDK1 and its phosphorylations were detected using mixtures of one phosphospecific CDK1 antibody (PT14, PT161, or PY15; green detection) and the A17 CDK1 monoclonal antibody (red detection) and revealed using mixed secondary antibodies coupled to DyLight 680 and 800. The infrared fluorescent emission from these dyes is visualized in red and green false colors, respectively. (B) Schematic representation of the total CDK1 pattern. The observed CDK1 forms are exactly positioned relative to a scale of isoelectric points (pI). Positions of computed isoelectric points resulting from the addition to CDK1 of entire numbers of negative charges are also shown. CDK1 forms are labeled according to their position and demonstrated phosphorylation(s) (e.g., 2P14,15 means CDK1 phosphorylated at both T14 and Y15; see the text for further explanation).

CDK2 forms, identified as previously (Coulonval *et al.*, 2003). In S/G2 cells, they were more abundant than CDK1 phosphoforms in cyclin A2 complexes, whereas they were undetectable in cyclin B1 complexes (Figures 3B and 4B). This confirms that CDK2 is the most abundant catalytic partner of cyclin A2 and is not physiologically associated with cyclin B1.

Cyclin A2-bound and cyclin B1-bound CDK1 consisted mainly of the fully phosphorylated 3P14,15,161 form. The active 1P161 form was detectable in cyclin A2 complexes during S phase, but it mostly appeared in association with both cyclins upon mitosis entry (Figures 3B and 4; see also Figure 5). The 2P14,161 form was also observed in both CDK1 complexes before mitosis, but 2P15,161 was only detected in cyclin A2-bound CDK1 (Figures 3B and 4B). Whereas cyclin A2-CDK1 consisted only of T161 phosphorylated forms and cyclin B1 complexes only contained a minor proportion of CDK1 that was not phosphorylated at T161, T161 phosphorylated forms were almost undetectable in free CDK1 (Figures 3B and 4A). This sharply contrasted with the abundant presence of 1P15 and 2P14,15 forms in free CDK1 but not in cyclin-bound CDK1. The presence of T161 phosphorylated forms only in cyclin-CDK1 complexes was consistent with the mutual dependence of cyclin B-CDK1 assembly and CDK1 phosphorylation by CAK (Larochelle *et al.*, 2007). On the other hand, the phosphorylation at Y15 and T14 of a large fraction of monomeric CDK1 was unexpected, as these phos-

phorylations by Wee1 and Myt1 also require CDK1 binding to cyclins (Solomon *et al.*, 1990, 1992; Meijer *et al.*, 1991; Parker *et al.*, 1991; Liu *et al.*, 1997).

Considering this surprising result and the different subcellular compartmentalization of CDK1 complexes and kinases, we wanted to further characterize the relationship between the different phosphorylations of CDK1 in preliminary subcellular fractionation experiments. Cytoplasm and structured elements, including nuclei, were separated by mild mechanical cell lysis in isotonic buffer, which was followed by 600 × g centrifugation. We did not add detergents (such as NP-40, which is commonly used in separations of nuclei) during those separations, because detergents extract soluble cyclin-CDK complexes from morphologically intact nuclei (unpublished data; Szepesi *et al.*, 1994). As judged from a marked enrichment of nuclear cyclin A2 and CDK7 in this pellet, and pure association of cytoplasmic tubulin α with the supernatant, efficient separations were achieved with low levels of both nuclear breakage and cytoplasmic contamination of the pellet (Figure S1, A and C). Nevertheless, the totality of the *cis*-Golgi matrix protein GM130 was also associated with the 600 × g pellet, which we thus better qualified as nuclear plus Golgi (N+G) fraction (Figure S1). This particulate fraction likely contained other structured cytoplasmic elements, such as centrosomes (Bailey *et al.*, 1989) and insoluble intermediate filament systems (Staufenbiel and Deppert, 1982) anchored to nuclear lamina (Georgatos and Blobel, 1987). Myt1 was almost exclusively found in the N+G fraction (Figure S1, A and C). On the other hand, the association of Wee1 with both fractions (Figure S1, A and C) was unlikely due to nuclear breakage and is consistent with recent reports of regulated Wee1 nuclear export (Katayama *et al.*, 2005; Li *et al.*, 2010).

Whereas the larger part of CDK1, including most of its nonphosphorylated form, was observed in T98G and HeLa cells in S and G2 phases in the cytoplasmic fraction, as expected (Bailey *et al.*, 1989), a large portion of cyclin B1 and most of the cyclin B1-CDK1 complexes were observed in the N+G fraction (Figure S1, A and C). This could be explained both by nuclear shuttling (Hagting *et al.*, 1999) and by the association of cyclin B1 and most of the cyclin B1-bound hyperphosphorylated CDK1 with insoluble cytoplasmic structures (Bailey *et al.*, 1989, 1992; Jackman *et al.*, 1995; Sanchez *et al.*, 2003). Two-dimensional separations of CDK1 in both HeLa and T98G cells showed again that T161 phosphorylation was mostly present as the hyperphosphorylated 3P14,15,161 form in cyclin B1-CDK1 complexes enriched in the N+G fraction. By contrast, most of cytoplasmic CDK1 was not associated with cyclin B1 and consisted of nonphosphorylated CDK1, 1P15 form and, less abundantly, 1P14 form (Figure S1, B and D). T14 phosphorylation was more prominent in the N+G fraction, especially in T98G cells. Fractionation and comparison of immunoprecipitations using CDK1 and cyclin B1 antibodies indicated that Y15 and T14 phosphorylations largely

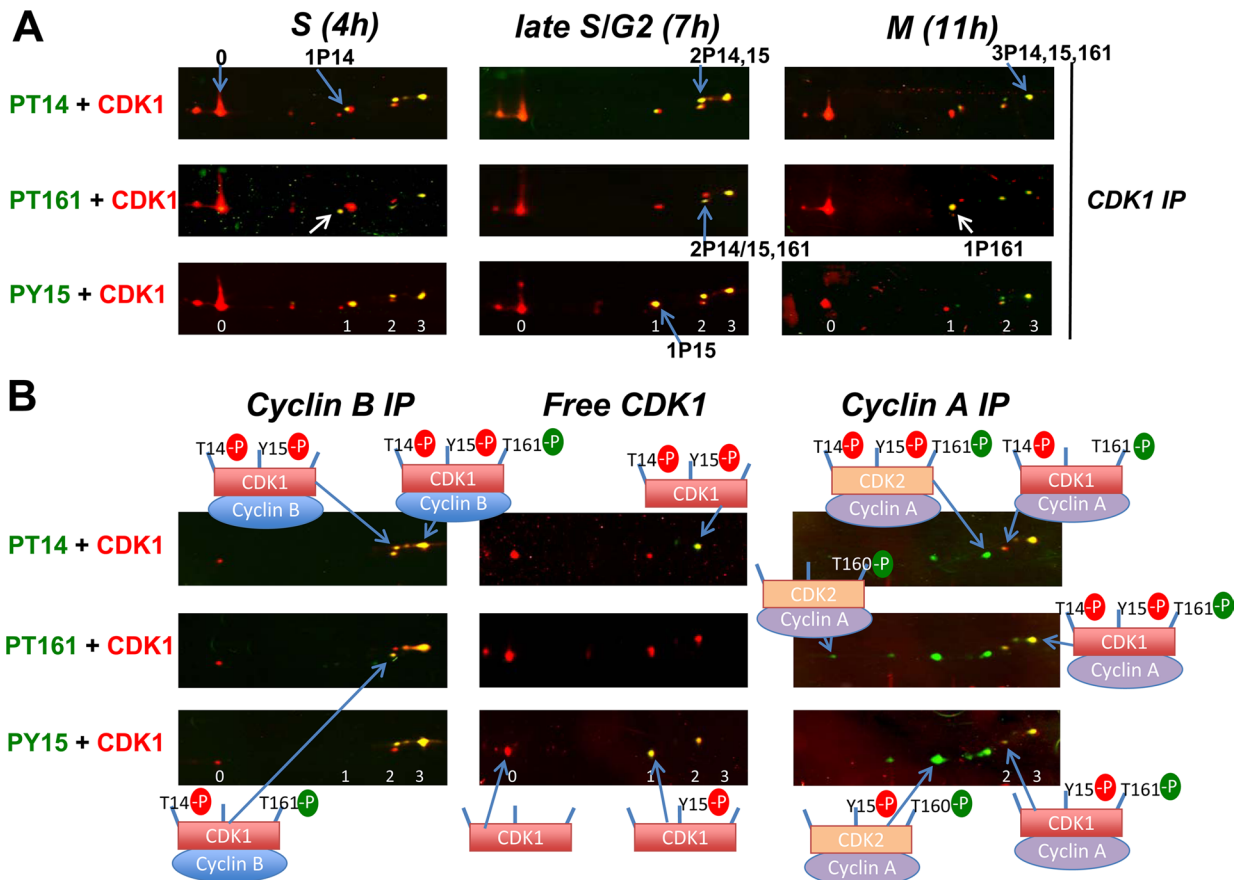


**FIGURE 3:** Double immunofluorescence analysis of CDK1 phosphoforms complexed or not with cyclins in synchronized HeLa cells. (A) Total CDK1 was immunoprecipitated with an anti-CDK1 antibody (C-19) from NP40 extracts of HeLa cells released from a double thymidine block and lysed at time points corresponding to S phase (4 h), late S/G2 (7 h), and mitosis (M; 11 h). The white arrow indicates the active single T161 phosphorylated form. (B) NP40 extracts from G2 phase HeLa cells were either immunodepleted from cyclin-bound CDK1 and then immunoprecipitated with the C19 anti-CDK1 antibody (free CDK1), or immunoprecipitated with anti-cyclin B1 or A2 antibodies (cyclin B IP, cyclin A IP). Immunofluorescence detections were performed as in Figure 2. The number of phosphorylation(s) of CDK1 is denoted 0, 1, 2, 3. In cyclin A IP, phosphospecific CDK1 antibodies also detected phosphorylated CDK2 forms, which appear in green.

occurred separately in monomeric CDK1 in both fractions, whereas their association was mostly found in the N+G fraction (Figure S1, B and D).

### Exclusive association of activating T161 phosphorylation and inhibitory T14 phosphorylation in cyclin B1–CDK1 complexes

In all of the above experiments, T161 phosphorylation before onset of mitosis was always associated with both cyclin binding and inhibitory phosphorylations. An analysis of the kinetics of CDK1 phosphorylation in cyclin B1 complexes (Figure 5) confirmed that the active 1P161 form was totally absent in G2 but appeared upon mitosis entry, even becoming the most prevalent form by far in cells blocked in prometaphase by colcemid (Figure 5B). Importantly, in both HeLa and T98G cells in S/G2 phase, T161 phosphorylation of cyclin B1-bound CDK1 exclusively occurred in association with the T14 phosphorylation in the 3P14,15,161 and less abundant 2P14,161 forms. Indeed, not only the 1P161 form but also the 2P15,161 form were absolutely undetectable in cyclin B1 complexes at this stage, that is, 7 h after release from the thymidine block in HeLa cells (Figure 5A) and 22 h after serum stimulation in T98G cells (Figure 5B). The 2P15,161 form only appeared (along with the 1P161 form) in cyclin B1 complexes at later time points (Figure 5, A and B), corresponding

to the maximal presence of mitotic cells (Figure 1). This form was thus most likely due to partial dephosphorylation of the 3P14,15,161 form. The exclusive association of T161 and T14 phosphorylations before onset of mitosis was specific for cyclin B1–CDK1 complexes. Indeed, small proportions of 1P161 and 2P15,161 form were detected in immunoprecipitation by CDK1 and cyclin A2 antibodies (Figures 3A and 4B). Figure 5C summarizes the CDK1 phosphoforms observed (and not observed) in S/G2 phases, and the shift in CDK1 phosphoforms occurring in cyclin B1 complexes during the G2/M transition, illustrating the strict association between T161 phosphorylation and both cyclin B1 binding and T14 phosphorylation.

### Knockdown of Wee1, but not Myt1, induces premature appearance of single T161-phosphorylated cyclin B1–CDK1 and catastrophic mitoses

The above observations might suggest that T14 phosphorylation by Myt1 could somehow prime CDK1 phosphorylation by CAK. However, previous mutagenesis experiments in different cells, including HeLa cells, have rejected this as a direct mechanism. Indeed, T14A and T14A,Y15F nonphosphorylatable CDK1 mutants are active and phosphorylated at T161 (Krek and Nigg, 1991a; Norbury et al., 1991; Pomerening et al., 2008; Potapova et al., 2009; Solomon et al., 1992). To evaluate the possibility of a mechanism that would



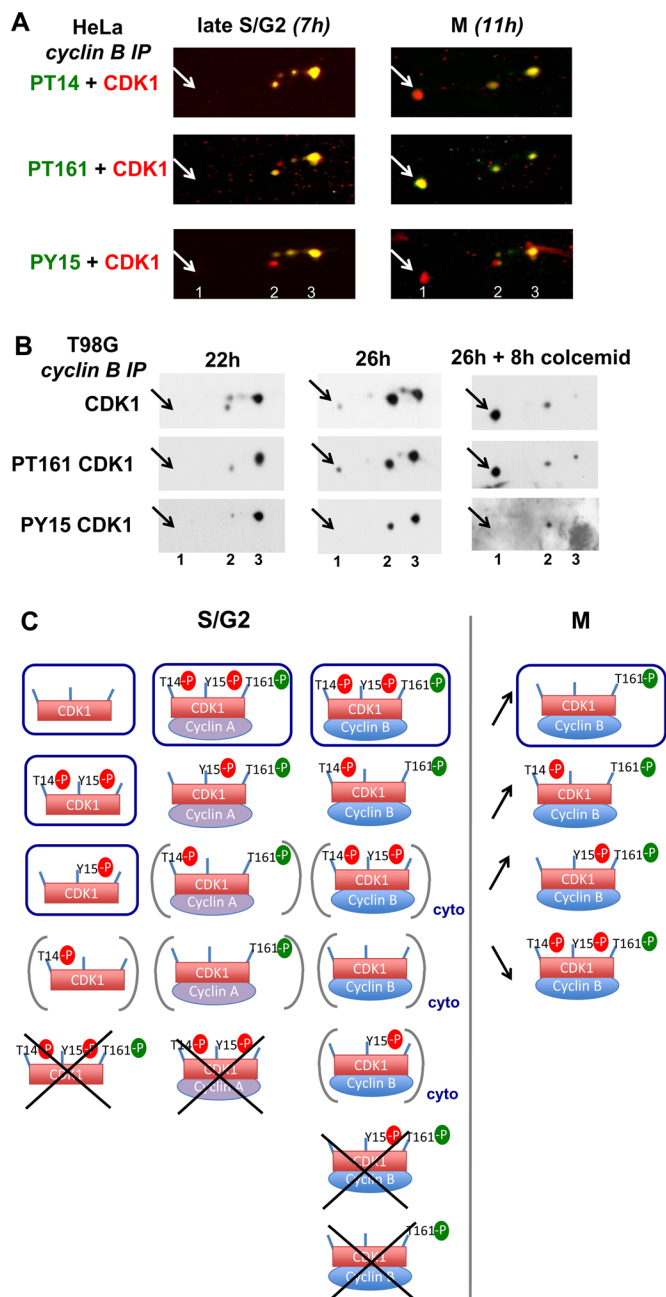


**FIGURE 5:** Strict association of T161 and T14 phosphorylations in cyclin B1-CDK1 complexes during G2 phase. (A) NP40 extracts from synchronized HeLa cells lysed at time points corresponding to late S/G2 phase (7 h) and mitosis (M; 11 h) were coimmunoprecipitated with anti-cyclin B1 antibody, separated by two-dimensional gel electrophoresis, and subjected to double immunofluorescence detection of CDK1 phosphoforms, as in Figure 2. (B) NP40 extracts from T98G cells stimulated with 15% serum for 22, 26, or 26 + 8 h with colcemid were coimmunoprecipitated with anti-cyclin B1 antibody and separated by two-dimensional gel electrophoresis. CDK1, phospho-T161 CDK1 and phospho-Y15 CDK1 were immunodetected. The pictures were taken as close-ups to show only the phosphoforms of CDK1. The number of phosphorylation(s) is denoted 1, 2, 3. The arrows indicate the position of the active single T161 phosphorylated form. (C) Cartoon summarizing the CDK1 phosphoforms observed in S/G2 phases and their association with cyclins, and the shift in CDK1 phosphoforms occurring in cyclin B1 complexes during the G2/M transition. The most abundant forms are circled; very minor but detectable forms are bracketed; some totally

completion of DNA replication. Importantly, combined knockdown of Myt1 and Wee1 attenuated, rather than augmented, the effects of the Wee1 siRNAs (Figure 6).

The impact of Myt1 and Wee1 siRNAs on the different CDK1 phosphorylations was examined by double immunofluorescence detections from SDS-PAGE separations (Figure 7A) and quantitated using the Odyssey scanner (Figure 7B), which provides direct and reliable measurements of the immunofluorescence detections independent of the adjustment of visualization parameters. Myt1 siRNAs substantially inhibited T14 phosphorylation but not Y15 phosphorylation. By contrast, Wee1 siRNAs strongly inhibited Y15 phosphorylation at all time points and also T14 phosphorylation after the release of the thymidine block (Figure 7, A and B). This delayed impact on T14 phosphorylation coincided, at 0 h and subsequent time points, with an almost complete shift of Myt1 toward its mitotic hyperphosphorylated forms (Figure 6A), which do not interact with cyclin B1-CDK1 complexes and hence do not phosphorylate CDK1 (Liu *et al.*, 1999). The decreased T14 phosphorylation induced by Wee1 knockdown was thus a secondary event resulting from the premature occurrence of mitoses. Despite the fact that Myt1 siRNAs slightly increased Wee1 protein levels, including in the absence of Wee1 siRNAs (Figure 6A), combined knockdown of Myt1 and Wee1 consistently reduced T14 and Y15 phosphorylations, as compared with the respective single knockdown of Wee1 and Myt1 (Figure 7, A and B).

In these experiments, the Myt1 siRNAs reduced the overall phosphorylation of CDK1 at T161 by ~40% (Figure 7, A and B), indicating that the activating phosphorylation of CDK1 somehow depends on Myt1 expression. This was similarly observed in cells treated with the combination of Myt1 and Wee1 siRNAs. By contrast, no such reduction of T161 phosphorylation was observed in cells treated with the Wee1 siRNAs alone (Figure 7, A and B).

Two-dimensional separations of CDK1 from cells treated with Wee1 siRNAs confirm that Y15 and T161 phosphorylations were not coupled (Figure 7C). In the CDK1 immunoprecipitate, the overall reduction in Y15 phosphorylation was reflected by a complete disappearance of 1P15 and 2P14,15 forms and a partial diminution of the cyclin-associated 3P14,15,161 form. As the T161 phosphorylation was not decreased, this reduction of 3P14,15,161 in the cyclin B1-CDK1 coimmunoprecipitate led to an increased proportion of the 2P14,161 form and appearance of the active 1P161 form (Figure 7C). This is the likely cause of the premature mitoses.

Treatment with Myt1 siRNAs similarly generated in CDK1 immunoprecipitate a strong reduction of 1P14 and 2P14,15 forms and a much more partial diminution of 3P14,15,161. However, in contrast with the situation generated by Wee1 knockdown, the reduction of T14 phosphorylation by Myt1 knockdown did not at all induce the appearance of 2P15,161 and active 1P161 form in cyclin B1 complexes (Figure 7C), likely due to concomitant reduction in T161 phosphorylation (Figure 7, A and B). This suggests an involvement of Myt1 not only in T14 phosphorylation but also in T161 phosphorylation of cyclin B1-CDK1 by CAK, leading to a tight coupling between T161 and T14 phosphorylations in cyclin B1-CDK1 complexes. This tight coupling appears to protect cells from premature cyclin B1-CDK1 activation and catastrophic mitoses, such as those provoked by Wee1 knockdown.

undetected forms are crossed out. cyto, forms that were detected only in cytoplasmic fraction. Arrows indicate the relative evolution of cyclin B1-bound CDK1 phosphoforms upon onset of mitosis.

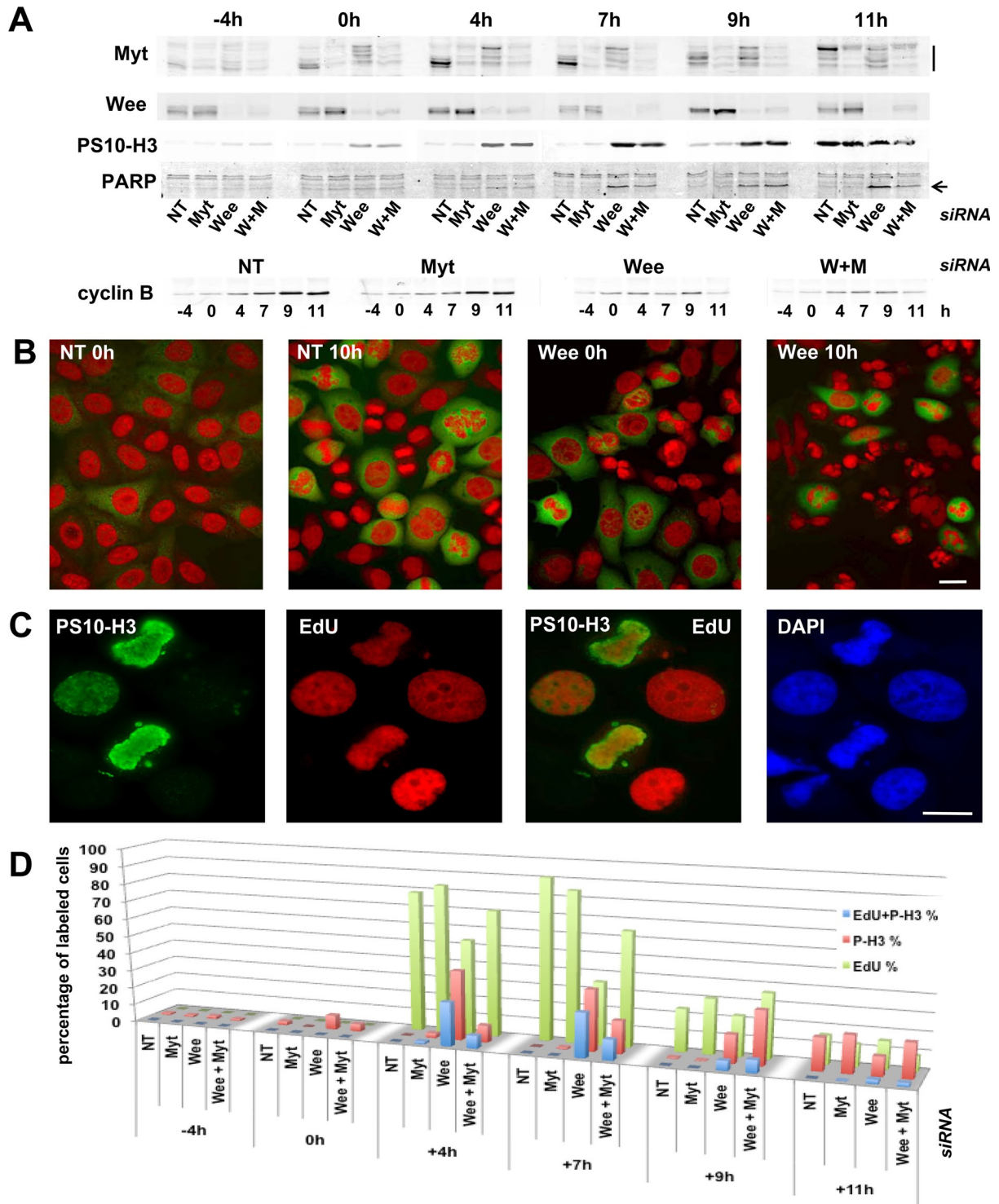


**FIGURE 6:** Knockdown of Wee1, but not of Myt1, induces catastrophic mitoses. Synchronized HeLa cells were transfected with the indicated siRNA pools in the interval between the two thymidine blocks and harvested at different time points before and after release (at 0 h) from the second block. NT, control nontargeting siRNA pool; W+M, combined transfection with Wee1 and Myt1 siRNA pools. (A) Whole-cell extracts were analyzed by SDS-PAGE, which was followed by immunoblotting with the indicated antibodies. The mobility shift of Myt1 is indicated by a vertical line. The arrow indicates the cleaved fragment of PARP. (B) HeLa cells transfected with NT or Wee1 siRNA pools and fixed 0 or 10 h after release from the last thymidine block. Cells were stained with anti-cyclin B1 antibody (green) and propidium iodide (red). Anomalous mitotic figures were observed in cells transfected with the Wee1 siRNA even during the thymidine block, which led a few hours later to a massive nuclear fragmentation. Scale bar: 10  $\mu$ m. (C) Wee1 siRNA-transfected cells, 4 h after thymidine block release. Anti-phosphohistone H3 staining (PS10-H3, green) appeared in DNA-replicating cells (EdU incorporation, red). Counterstaining with 4',6-diamidino-2-phenylindole (DAPI). Scale bar: 10  $\mu$ m. (D) Percentages of DNA-replicating cells (EdU incorporation), phosphohistone H3 (P-H3)-positive cells, and cells positively stained for both phosphohistone H3 and EdU incorporation. More than 400 cells were counted in each condition.

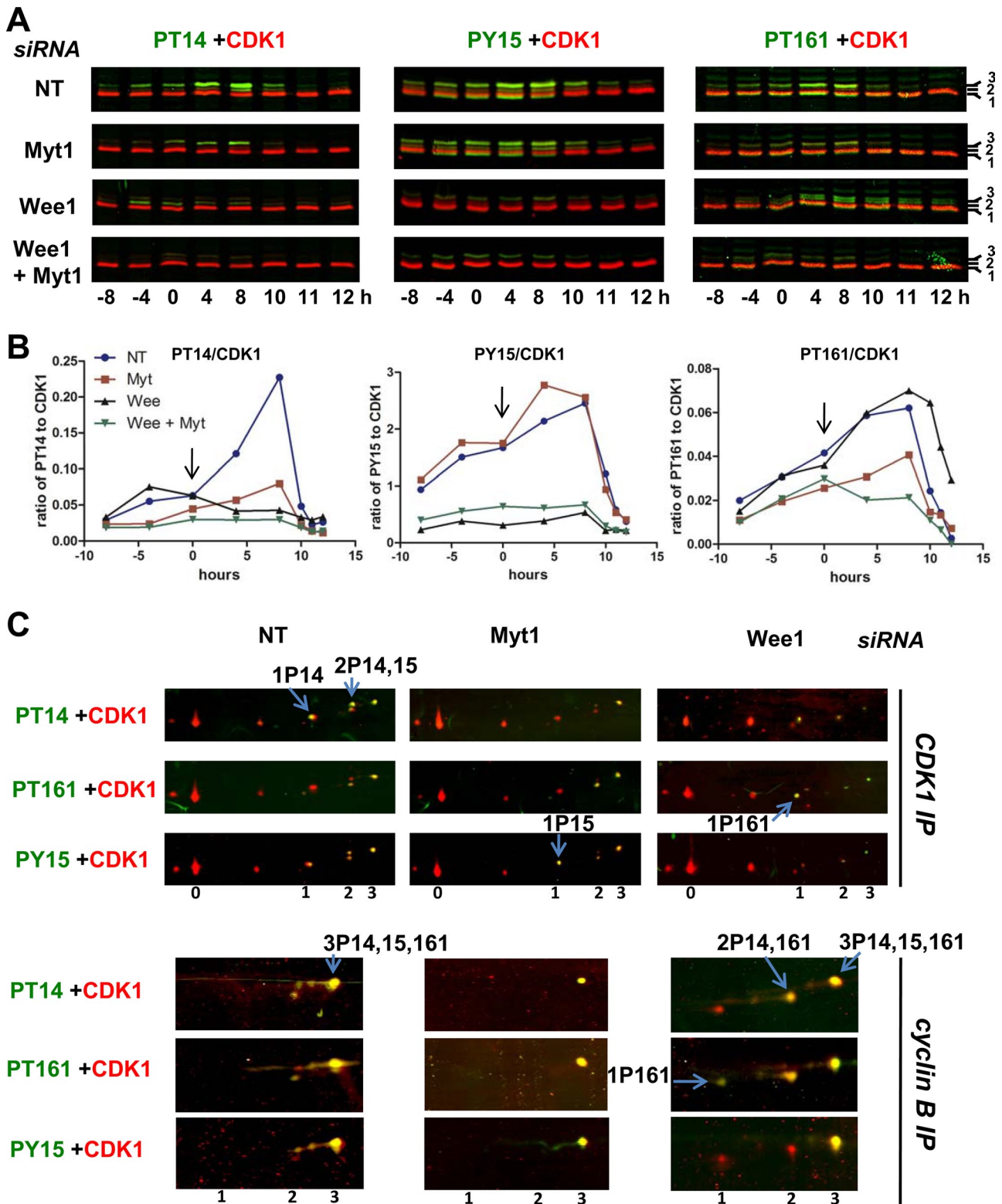


**FIGURE 7:** Impact of Myt1 and Wee1 knockdown on CDK1 phosphorylations. Synchronized HeLa cells were treated with the indicated siRNA pools, as in Figure 6. (A) Whole-cell extracts were analyzed by SDS-PAGE, which was followed by double immunofluorescence detection of CDK1 (red false color) and phospho-T14, -T161 or -Y15 CDK1 (green false color). CDK1 separated in three bands (1, 2, 3). (B) The ratios of fluorescences corresponding to phosphorylated CDK1 (bands 2 and 3, channel 800) and total CDK1 (channel 680) from the blots illustrated in (A) were quantified using the Odyssey infrared fluorescence scanner. (C) Extracts from siRNA-transfected HeLa cells harvested 7 h (S/G2 phase) after the second thymidine release were either immunoprecipitated with an anti-CDK1 antibody (CDK1 IP, denatured lysates) or with an anti-cyclin B1 antibody (cyclin B IP, NP40 lysates), separated by two-dimensional gel electrophoresis, and subjected to double immunofluorescence detection of CDK1 phosphoforms, as in Figure 2. In each condition, most characteristic CDK1 forms are indicated by arrows.

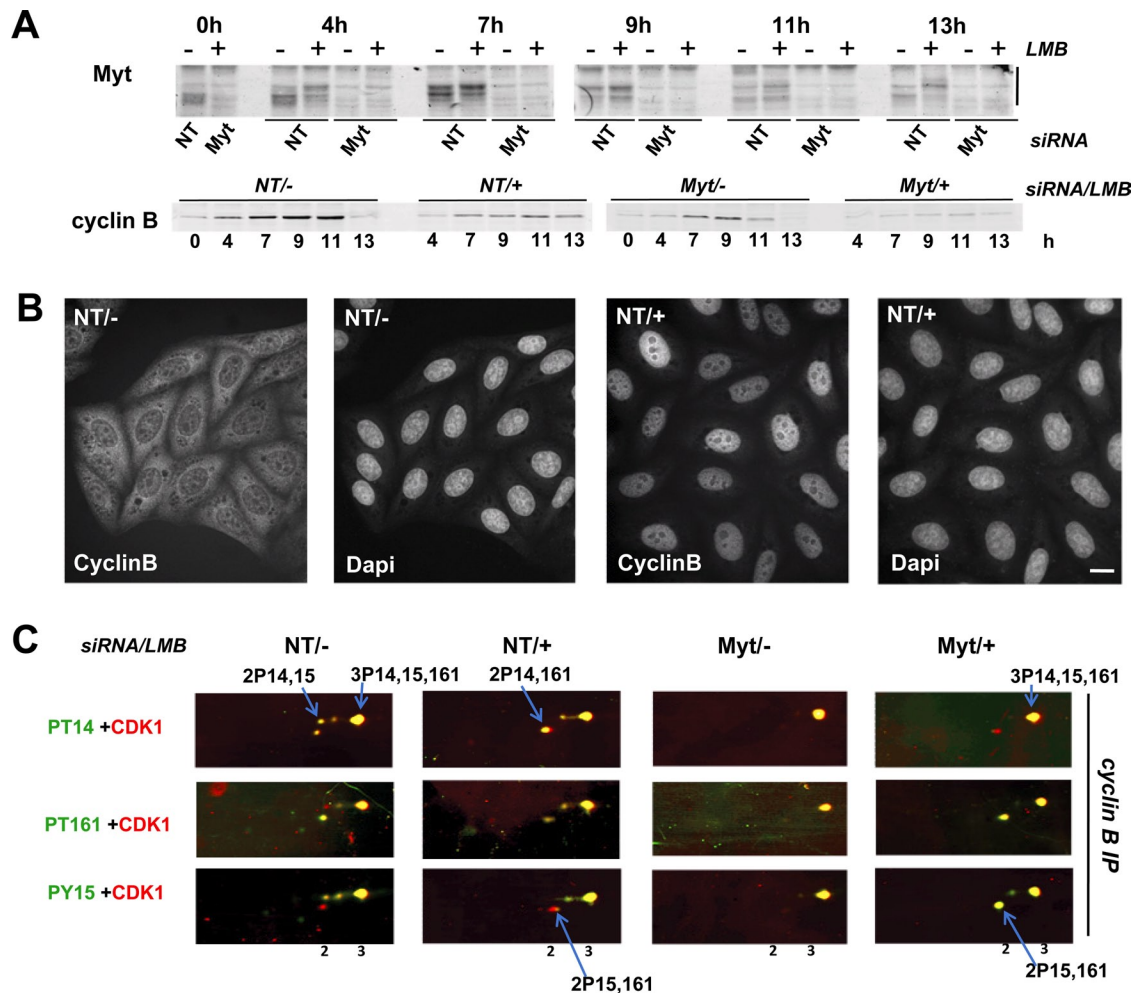


**FIGURE 8:** LMB treatment uncouples T161 and T14 phosphorylations in cyclin B1-CDK1 complexes. Synchronized HeLa cells were treated with the indicated siRNA pools (NT, control nontargeting siRNA pool), as in Figure 6. At time 0 (second release), cells were either left untreated (–) or incubated with 30 nM LMB (+). (A) Whole-cell extracts were analyzed by SDS-PAGE, which was followed by immunoblotting with the indicated antibodies. The mobility shift of Myt1 is highlighted. (B) HeLa cells transfected with NT siRNA pool, treated (+) or not (–) with LMB, and fixed 7 h after release from the last thymidine block. Cells were stained with anti-cyclin B1 antibody and counterstained with DAPI. Scale bar: 10  $\mu$ m. (C) Extracts from siRNA-transfected HeLa cells harvested 7 h after the second thymidine release were immunoprecipitated with an anti-cyclin B1 antibody (*cyclin B IP*, NP40 lysates), separated by two-dimensional gel electrophoresis, and subjected to double immunofluorescence detection of CDK1 phosphoforms, as in Figure 2. In each condition, most characteristic CDK1 forms are indicated by arrows.

### The coupling between T161 and T14 phosphorylations depends on unperturbed traffic of cyclin B1-CDK1

We were intrigued by the observation that the partial Myt1 knock-down much more strongly reduced 1P14 and 2P14,15 forms than the 3P14,15,161 one (Figure 7C). This suggested that reduced Myt1 expression also increased the recruitment of cyclin B1-CDK1 to nuclear phosphorylation by CAK. Myt1 is anchored in the ER and Golgi complex (Booher *et al.*, 1997; Liu *et al.*, 1997) and previous studies have demonstrated that its interaction with cyclin B1-CDK1 is strong enough to explain that Myt1 overexpression, even as a kinase-inactive form, can slow down G2/M progression by impairing the nuclear import of cyclin B1-CDK1 (Liu *et al.*, 1999; Wells *et al.*, 1999). We were therefore also envisaging that Myt1 could play separate roles in phosphorylating cyclin B1-CDK1 at T14 and influencing its traffic to the nucleus and hence its phosphorylation at T161 by CAK (see *Discussion*). If this possibility were true, forcing a nuclear colocalization of cyclin B1-CDK1 and CAK using the CRM1 ex-

portin inhibitor leptomycin B (LMB; Hagting *et al.*, 1998; Yang *et al.*, 1998; Liu *et al.*, 1999) might uncouple T161 and T14 phosphorylations.

Synchronized HeLa cells were transfected with Myt1 or nontargeting siRNAs, as in Figures 6 and 7, and released from the thymidine blocks in the presence or absence of LMB. As shown in Figure 8, A and B, Myt1 siRNAs efficiently reduced Myt1 expression both in the presence and absence of LMB, and LMB treatment induced an exclusive nuclear location of cyclin B1. Seven hours after release of the thymidine block, when most cells were in late S/early G2 phase regardless of treatment (Figure S2C), phosphorylations of cyclin B1-bound CDK1 were studied using two-dimensional electrophoresis (Figure 8C). Both Myt1 siRNAs (as also seen in Figure 7C) and LMB induced the disappearance of the 2P14,15 form, but not of the 3P14,15,161 form, consistent with a more complete recruitment of cyclin B1-CDK1 for phosphorylation by CAK. A minor presence of the 2P15,161 form was detected in

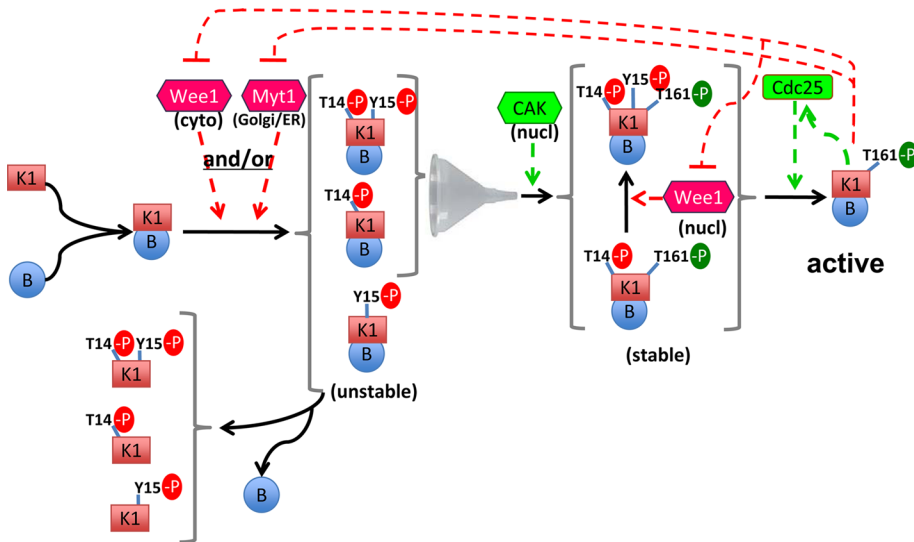


**FIGURE 9:** Ordering cyclin binding and phosphorylations in cyclin B1–CDK1 activation. Cyclin B1–CDK1 is continuously shuttling but mostly cytoplasmic, due to its more active nuclear export. Our data suggest that upon binding to cyclin B1, nonphosphorylated CDK1 can be immediately phosphorylated by Wee1 and/or Myt1, but not by nuclear CAK. In the absence of T161 phosphorylation, these cyclin B1–CDK1 complexes are unstable and therefore release the observed monomeric CDK1 phosphorylated at Y15 and/or T14. We also unexpectedly observed here that the T161 phosphorylation of CDK1 by CAK does not occur without the T14 phosphorylation and depends on Myt1 expression. We propose that the previously demonstrated interaction of cyclin B1–CDK1 with Myt1 anchored in ER and Golgi membranes would be required not only for T14 phosphorylation of CDK1, but also to somehow prime its T161 phosphorylation by CAK in nucleus. We hypothesize that this interaction with Myt1, which has been shown to be transient and regulated, might address T14-phosphorylated cyclin B1–CDK1 to a traffic pathway that channels it for phosphorylation by CAK. The observations that cyclin B1–CDK1 is not freely diffusible in cytoplasm, and that the dependence of T161 phosphorylation on Myt1 was abrogated by the forced nuclear colocalization of cyclin B1–CDK1 with CAK, support such a mechanism. The observed tight coupling of T161 and T14 phosphorylations protects cyclin B1–CDK1 from premature activation and ensures that it is only activated by dephosphorylation by Cdc25 phosphatases (depending on nuclear export, as cyclin B1–CDK1 is first activated on centrosomes).

LMB-treated cells (Figure 8C), reminiscent of the situation observed in nuclear cyclin A–CDK1 complexes (Figures 3B and 4B). Moreover, in the presence of LMB, but not in its absence, Myt1 knockdown induced a massive increase of the proportion of this 2P15,161 form (Figure 8C). Importantly, no 1P161 form was detected at this time point, consistent with the absence of mitotic cells (Figure S2C). These observations confirmed that T161 phosphorylation can occur without T14 phosphorylation (Krek and Nigg, 1991a; Norbury *et al.*, 1991; Solomon *et al.*, 1992). Moreover, they indicate that the tight coupling between T161 and T14 phosphorylations observed in cyclin B1–CDK1 requires a properly functioning cytoplasm–nucleus traffic.

As previously reported (Yoshida *et al.*, 1990), LMB prevented the entry of cells in mitosis, as shown by lack of both mitotic figures and phosphohistone H3 detection (Figure S2). Because no 1PT161 CDK1 was observed, dephosphorylation of CDK1 by Cdc25 phosphatases was likely impaired, consistent with evidence that these phosphatases first activate cyclin B1–CDK1 in cytoplasm (Gavet and Pines, 2010a; Jackman *et al.*, 2003). Interestingly, whereas Myt1 knockdown did not accelerate onset of mitosis in the absence of LMB (Figures 6 and S2), it did partially rescue the LMB-induced G2 arrest, as shown by the appearance of mitoses at 11 and 13 h (Figure S2, A–C). The large occurrence in cyclin B1 complexes of CDK1 phosphorylated at T161 and Y15, but not T14, as resulting from the uncoupling of T161 and T14 phosphorylations by reduced

Myt1 expression in LMB-treated cells (Figure 8C), might thus ultimately facilitate cyclin B1–CDK1 activation.

## DISCUSSION

The sequence of events leading to the accumulation in G2 phase of the reservoir of fully phosphorylated cyclin B1–CDK1 complexes remains unclear. The three Y15, T14, and T161 phosphorylations depend on CDK1 binding to a cyclin (A or B type), and thus would coincide with the accumulation of these cyclins and formation of their complex with CDK1. However, this scenario appears too simplistic in view of the various compartmentalizations of the cyclin–CDK1 complexes and their kinases. Moreover, such a model must be reconciled with evidence that the stable assembly of cyclin B1 and CDK1 requires its T161 phosphorylation by CAK but not inhibitory phosphorylations (Ducommun *et al.*, 1991; Larochelle *et al.*, 2007; Merrick *et al.*, 2008), which might imply that inhibitory phosphorylations are dependent on—and thus occur after—the activating phosphorylation. Such a “reverse” sequence of phosphorylation events would not preclude a temporary occurrence of fully active single T161 phosphorylated cyclin B1–CDK1. Owing to various positive and double negative feedback loops, this is known to trigger the explosive activation of the whole pool of cyclin B1–CDK1, which is catastrophic when occurring prematurely.

Our analysis demonstrates the physiological occurrence of the seven possible CDK1 phosphoforms that combine the T14, Y15, and/or T161 phosphorylations. Most importantly, it resolves for the first time whether CDK1 phosphorylated at Y15 and/or T14 is also phosphorylated at T161. Our data directly confirm that the activating T161 phosphorylation of cyclin B1–bound CDK1 is restricted in interphase to CDK1 maintained in an inactive state by inhibitory phosphorylations and that the activation at mitosis of the whole pool of cyclin B1–CDK1 complexes results only from dephosphorylation of Y15 and T14 residues. Novel findings that could be obtained only thanks to the two-dimensional electrophoresis approach include: 1) the abundant detection of Y15 and T14 phosphorylations in monomeric CDK1, at variance with cyclin-associated T161 phosphorylation; and 2) the tight coupling of T161 and T14 phosphorylations in cyclin B1–CDK1 complexes. In the following discussion, we examine how these data can be integrated with previous observations into a coherent working model (Figure 9).

### Inhibitory phosphorylations are not restricted to cyclin-bound CDK1 and likely precede the activating phosphorylation

T161 phosphorylation was observed only in cyclin-bound CDK1 and, conversely, the totality of CDK1 complexed to cyclin A2 and a large majority of cyclin B1–CDK1 complexes were phosphorylated at T161. This is consistent with the mutual dependence of the activating phosphorylation by CAK and cyclin–CDK1 assembly in stable complexes (Larochelle *et al.*, 2007). Moreover, the absence of T161

phosphorylation in monomeric CDK1 was likely to be due to dephosphorylation by T161-phosphatases, such as some phosphatase 2C isoforms (Cheng *et al.*, 2000) and CDK-associated phosphatase (KAP; Poon and Hunter, 1995), which do not act on cyclin-bound CDKs. Only a fraction of the minor proportion of cytoplasmic cyclin B1–CDK1 complexes that do not cosediment with the N+G fraction (see *Results*) also occurred without T161 phosphorylation, perhaps due to lack of access to nuclear CAK.

In contrast, the abundant phosphorylation of monomeric CDK1 at Y15 and T14 in both HeLa and T98G cells in G2 would suggest that, unexpectedly, CDK1 might be phosphorylated *in vivo* at Y15 and T14 independently of prior cyclin binding. Similarly, monomeric CDK2 is abundantly phosphorylated at Y15 in human fibroblasts (Coulonval *et al.*, 2003b). However, a more plausible explanation is compatible with both our results and *in vitro* experiments showing that Wee1 and Myt1 only phosphorylate cyclin-bound CDK1 (Solomon *et al.*, 1990, 1992; Meijer *et al.*, 1991; Parker *et al.*, 1991; Liu *et al.*, 1997). CDK1 could be phosphorylated by Wee1 and Myt1 when transiently associated with cyclin B1, which could be facilitated by the interaction of cyclin B1–CDK1 with these kinases (Liu *et al.*, 1999; Wells *et al.*, 1999; Deibler and Kirschner, 2010), and if those cyclin B1–CDK1 complexes are not stabilized by T161 phosphorylation (because of insufficient shuttling to nucleus and access to CAK), they would then release Y15/T14 phosphorylated monomeric CDK1 that would accumulate mainly in the cytoplasm (Figure 9). Whatever the explanation, the occurrence of T161 phosphorylation in only a subset of T14 + Y15-phosphorylated CDK1 demonstrates that T14 and Y15 phosphorylations do not depend on—and thus would not occur after—the stable assembly of cyclin–CDK1 complexes associated with the activating phosphorylation.

### **T14 phosphorylation by Myt1 appears to prime the T161 phosphorylation of cyclin B1–CDK1**

Perhaps the most intriguing novel finding is the observation that T161 phosphorylation never occurred without the inhibitory T14 phosphorylation in cyclin B1-bound CDK1. This strict association could not be uncoupled by a 60% reduction of overall T14 phosphorylation in response to partial Myt1 knockdown, indicating some causal relationship. Interestingly, this coupling was specific for cyclin B1–CDK1. Whereas this *apparent* priming effect of T14 phosphorylation by Myt1 on T161 phosphorylation by CAK obviously serves to prevent premature activation of cyclin B1–CDK1, a mechanism(s) that can so selectively restrict cyclin B1–CDK1 phosphorylation by nuclear CAK to its T14 phosphorylated forms is not easily conceived (Figure 9). In fact, the coupling between both phosphorylations, as well as the T161 phosphorylation dependence on Myt1, could be disrupted by forced nuclear colocalization of cyclin B1–CDK1 and CAK using the exportin inhibitor LMB (Figure 8). T14 phosphorylation was thus not directly required for the recognition of cyclin B1–CDK1 by CAK, as demonstrated by previous studies showing that T14A and T14A,Y15F CDK1 mutants are active and phosphorylated at T161 (Krek and Nigg, 1991a; Norbury *et al.*, 1991; Solomon *et al.*, 1992; Jin *et al.*, 1998; Pomerening *et al.*, 2008; Potapova *et al.*, 2009). Therefore our data show that cyclin B1–CDK1 phosphorylation by CAK somehow depends on Myt1 expression, but not on T14 phosphorylation itself, and that this dependence requires the unperturbed intracellular traffic of cyclin B1–CDK1.

How could this be envisaged mechanistically? Throughout interphase, cyclin B1–CDK1 shuttles between the cytoplasm and nucleus, but is mostly cytoplasmic, because its nuclear import is slower than its export (Hagting *et al.*, 1998; Yang *et al.*, 1998; Moore *et al.*, 1999). Nevertheless, cyclin B1–CDK1 complexes do

not freely diffuse in the cell, at variance with monomeric CDK1 (Bailey *et al.*, 1989, 1992; Jackman *et al.*, 1995). These complexes were mainly found together with the *cis*-Golgi/ER proteins GM130 and Myt1 in our N+G fraction. T14 phosphorylation is performed only by Myt1, which is anchored in the ER and Golgi complex (Booher *et al.*, 1997; Liu *et al.*, 1997). This requires a specific interaction between cyclin B1 and the C-terminus of Myt1, depending on its RXL motif (Liu *et al.*, 1999; Wells *et al.*, 1999; Ruiz *et al.*, 2010). When Myt1 is overproduced, even as a kinase-inactive form, this interaction is strong enough to interfere with the intracellular trafficking of cyclin B1–CDK1 (Liu *et al.*, 1999; Wells *et al.*, 1999). However, under physiological conditions, the cyclin B–Myt1 interaction, which can be regulated by Myt1 phosphorylations, must be fairly transient to allow the continuous shuttling of cyclin B1 complexes (Liu *et al.*, 1999; Ruiz *et al.*, 2010). In keeping with those previous reports, we thus propose that cytoplasmic cyclin B1–CDK1 must first bind (at least transiently) to Golgi/ER-anchored Myt1—demonstrated by T14 phosphorylation—to be addressed for phosphorylation by CAK in nucleus. In other words, the observation that T161 phosphorylation did not occur without T14 phosphorylation indicates that all T161-phosphorylated cyclin B1–CDK1 complexes had first to interact with Myt1, which thus appears to be a rate-limiting step for priming phosphorylation by CAK. Therefore Myt1 might have a central role not only in inhibiting CDK1 through T14 phosphorylation but also in addressing cyclin B1–CDK1 to a trafficking process that selectively delivers it to nuclear CAK (Figure 9). Given that Myt1 has the capacity to both phosphorylate cyclin B1–CDK1 and retain it on ER and Golgi complex membranes, its partial knockdown would not only reduce T14 phosphorylation of cyclin B1–CDK1 but also accelerate its nuclear import. This was indeed observed, since the reduction of overall T14 phosphorylation induced by Myt1 siRNAs was paradoxically associated with a much more complete recruitment of T14 phosphorylated forms to T161 phosphorylation, as reflected by the strong reduction of 1P14 and 2P14,15 forms with a more partial diminution of the hyperphosphorylated 3P14,15,161 form (Figure 7C). More extensive ultrastructural and biochemical studies will be required to understand the traffic of endogenous cyclin B1–CDK1 after its interaction with Myt1 and T14 phosphorylation, most likely along membranes of the ER, which are continuous with the nuclear envelope and nuclear pores.

### **How exactly does Wee1 knockdown induce the premature activation of cyclin B1–CDK1?**

Based on transfection experiments, it has been proposed that human Wee1 maintains mitotic timing by protecting the nucleus from cytoplasmically activated CDK1 (Heald *et al.*, 1993). However, this mechanism is unlikely to be physiological, because our results totally failed to detect the single T161 phosphorylated cyclin B1–CDK1 in cytoplasm and the product of its phosphorylation by Wee1 in nucleus (the cyclin B1-bound 2P15,161 CDK1 form) before onset of mitosis.

Wee1 knockdown led, as expected, to a strong reduction of all the Y15 phosphorylated CDK1 forms. No coupling between phosphorylations at Y15 and T161 was observed, and, as a result, T161 phosphorylation was largely found in cyclin B1–CDK1 complexes phosphorylated at T14 but not Y15. Nevertheless, this would not suffice to explain the appearance of the active single T161 phosphorylated cyclin B1–CDK1 that likely causes the premature mitotic events. Interestingly, a previous analysis of T14A, Y15F, and double T14AY15F CDK1 mutants in HeLa cells has suggested that T14 phosphorylation substantially delays CDK1 activation but does not completely prevent it, unlike Y15 phosphorylation (Krek

and Nigg, 1991b). Therefore cyclin B1–CDK1 complexes phosphorylated at T161 and T14, but not at Y15 (2P14,161 form), would retain some activity that, when their presence is increased by down-regulation of Wee1, would suffice to trigger activating feedback loops involving Cdc25 phosphatases. Moreover, Wee1 knockdown also markedly reduced the Y15 phosphorylation of CDK2 without decreasing its T160 phosphorylation (unpublished data). As most cyclin A-bound T160 phosphorylated CDK2 is phosphorylated at Y15 but not T14 (Coulonval *et al.*, 2003; see also Figures 3B and 4B), reducing its Y15 phosphorylation should considerably activate the complex. Consistent with evidence that cyclin A–CDK2 primes the activation of cyclin B1–CDK1 (Fung *et al.*, 2007; Furuno *et al.*, 1999), decreased Y15 phosphorylation of cyclin A2–CDK2 might thus contribute to activate cyclin B1–CDK1 by activating Cdc25 phosphatases (Fung *et al.*, 2007). In the present study, and in the Nakajima *et al.* (2008) study, the impact on mitotic timing of Wee1 siRNAs administered after the first thymidine block appeared more dramatic than the phenotype observed by others after CDK1AF expression in HeLa cells (Blasina *et al.*, 1997; Jin *et al.*, 1998). Whether this difference could be explained by the wider impact of Wee1 knockdown on the different CDK1 and CDK2 complexes should be further investigated. Finally, it must be mentioned that Wee1 knockdown also generates other major cell cycle perturbations, including defective mitosis exit followed by shorter G1 and S phases (Pomerening *et al.*, 2008), which might render cells more vulnerable to partially deregulated CDK1 activation, thus possibly exaggerating the occurrence of catastrophic mitoses.

Partial knockdown of Myt1 also had the capacity to accelerate onset of mitosis, but this required the uncoupling of T161 and T14 phosphorylations by LMB treatment (Figures 8C and S2). However, in a normal situation (without LMB), Myt1 knockdown did not augment the impact of Wee1 silencing in our experiments, contrasting with the notion of the double block to CDK1 activation provided by combined Y15 and T14 phosphorylations (Krek and Nigg, 1991b; Norbury *et al.*, 1991). Instead, combined Myt1 knockdown even attenuated the appearance of premature mitoses during Wee1 siRNA treatment (Figure 6), most likely because it also reduced T161 phosphorylation of CDK1 (Figure 7, A and B). This again underscores the gatekeeper role we propose for Myt1 in not only phosphorylating cyclin B1–CDK1 at T14 but also selectively addressing it for its T161 phosphorylation by CAK.

To conclude, our study has provided new insights about the intricate relationship between the various (de)phosphorylations of CDK1 that govern mitosis and its dependence upon completion of DNA replication. The unexpected observation that the activating phosphorylation of cyclin B1–CDK1 is tightly coupled to its T14 inhibitory phosphorylation suggests that the mitotic timer is endowed with an intrinsic mechanism protecting it from premature activation by constitutively active CAK. The absence of a similar coupling between T161 and Y15 phosphorylations explains why catastrophic mitoses are provoked by reduced expression of Wee1 but not of Myt1. The present methodology should prove a valuable experimental tool in any future investigation of CDK1 regulation.

## MATERIALS AND METHODS

### Cell culture, synchronization, and transfection

T98G cells (American Type Culture Collection) and HeLa cells were grown and maintained in DMEM supplemented with 10% fetal bovine serum (FBS). T98G cells were starved in 0.2% FBS for 3 d and then growth-stimulated by addition of 15% FBS. In some conditions, T98G cells were blocked in prometaphase by an 8-h colcemid treat-

ment (1  $\mu\text{g}/\text{ml}$ ), and rounded cells were detached by shake-off. HeLa cells were synchronized at the G1/S boundary by a double-thymidine block involving incubation with 2 mM thymidine for 16 h, release by rinsing with phosphate-buffered saline (PBS) and culture for 11 h in fresh medium, then a second block for 15 h with thymidine and release in fresh medium (time 0 h). For transfections with siRNA pools,  $2.5 \times 10^4$  cells/cm<sup>2</sup> were plated in 3- or 9-cm dishes for 48 h in antibiotic-free medium before the first thymidine block. Cells were transfected immediately after the first thymidine block in serum-free DMEM by adding siRNA pool lipid complexes (50 nM of a single siRNA pool, 2  $\mu\text{l}/\text{ml}$  DharmaFECT1 per pool; Dharmacon, Thermo Scientific, Lafayette, CO) according to the manufacturer's instructions. Ten percent FBS was added 4 h later. ON-TARGETplus SMARTpools (Dharmacon) were used against human PKMYT1 (Myt1; NM\_004203) and human WEE1 (Wee1; NM\_003390). Control was 50 nM of a nontargeting siRNA pool. In some experiments, synchronized HeLa cells were treated with 30 nM LMB (Santa Cruz Biotechnology, Santa Cruz, CA) or with vehicle (ethanol).

### EdU and BrdU incorporation

DNA-replicating cells were identified by a prior harvesting incubation either for 30 min with BrdU ( $10^{-4}\text{M}$ ) as described (Coulonval *et al.*, 2003a) or for 1 h with EdU (40  $\mu\text{M}$ ; Invitrogen, Carlsbad, CA). EdU-labeled cells were fixed with 3.7% paraformaldehyde for 15 min. Detection of EdU incorporation into DNA was performed with the Click-iT EdU Alexa Fluor 594 Cell Proliferation Assay kit (Invitrogen) according to the manufacturer's instructions.

### Indirect immunofluorescence

Cells in 3-cm Petri dishes were fixed with 2% paraformaldehyde for 90 s at 4°C and then methanol for 10 min at  $-20^\circ\text{C}$  and permeabilized with 0.1% Triton X-100 before immunofluorescence detection (Baptist *et al.*, 1996). Anti-cyclin B1 monoclonal (GNS1; Neomarkers, Fremont, CA) and anti-phosphohistone H3 (Ser10) polyclonal (Cell Signaling Technology, Danvers, MA) antibodies were detected using a biotinylated anti-mouse or rabbit immunoglobulin antibody and fluorescein-conjugated streptavidin.

### Cell fractionation

Cells were washed with cold  $\text{Ca}^{2+}/\text{Mg}^{2+}$ -free PBS and incubated on ice for 10 min with the following buffer (10 mM HEPES, pH 7.9, 1.5 mM  $\text{MgCl}_2$ , 10 mM KCl, 300 mM sucrose, 5% Ficoll, 1 mM EDTA, 0.25 mM ethylene glycol tetraacetic acid [EGTA], 50 mM NaF, 1 mM Na orthovanadate, protease inhibitors [pefablock, leupeptin], and 10% glycerol) and scraped. Cells were broken by mild mechanical homogenization (glass/glass), after which nuclei and some particulate material, including Golgi complex (see *Results*), were pelleted by centrifugation at  $600 \times g$  and 4°C for 10 min. This pellet was washed once with PBS and resuspended in the appropriate buffers for SDS-PAGE or immunoprecipitation. To the supernatant (cytoplasmic fraction), 5X Laemmli buffer or 0.5% NP40 was added for SDS-PAGE or immunoprecipitation.

### Immunoprecipitations

For the analysis of protein complexes, cells were lysed and homogenized in 1 ml NP-40 (0.5%) lysis buffer as previously described (Coulonval *et al.*, 2003b). Precleared cellular lysates were incubated at 4°C for 3 h with protein A-Sepharose (GE Healthcare, Waukesha, WI), which had been preincubated overnight with 2  $\mu\text{g}$  of one of the following antibodies: polyclonal anti-CDK1 (C19 or PSTAIRE, Santa Cruz Biotechnology), monoclonal antibodies against CDK1 (A17,

kindly gifted by Tim Hunt or from Neomarkers), cyclin B1 (GNS1) and cyclin A2 (E72) (both from Neomarkers). Alternatively, denatured lysates were prepared as described previously (Coulonval *et al.*, 2003b) for the analysis of total CDK1.

### Gel electrophoresis and Western blotting

For two-dimensional gel electrophoresis separations, immunoprecipitated proteins were denatured in a buffer containing 7 M urea and 2 M thiourea. Proteins were separated by isoelectric focusing using the Protean IEF cell (Bio-Rad, Hercules, CA) after active in-gel rehydration, as described previously (Coulonval *et al.*, 2003b), on immobilized linear pH gradient (pH 3–10) strips (GE Healthcare). After loading onto SDS-polyacrylamide slab gels (12.5%) for separation according to molecular mass, proteins were transferred to polyvinylidene fluoride (PVDF) membranes. CDK1 was immunodetected using polyclonal antibodies against CDK1 (C19 or PSTAIRE; Santa Cruz Biotechnology) and phospho-CDK1 (T14, T161, or Y15; Cell Signaling Technology) as previously described (Coulonval *et al.*, 2003b), which was followed by horseradish peroxidase-coupled secondary antibody for detection by enhanced chemiluminescence (Western Lightning; Perkin Elmer-Cetus, Waltham, MA). Alternatively, for double immunofluorescence detection using the Odyssey infrared fluorescence scanner (LI-COR Biosciences, Lincoln, NE), immunoprecipitated proteins were transferred to low-fluorescence PVDF membranes (Millipore, Billerica, MA) and CDK1 and its phosphorylated forms were detected using a mixture of the A17 monoclonal CDK1 antibody and one of the phospho-CDK1 antibodies diluted in the LI-COR blocking buffer. After washings, membranes were incubated with mixed anti-mouse and anti-rabbit secondary antibodies coupled to DyLight 680 and 800 (Perbio Science, Erembodegem, Belgium), respectively.

Whole-cell extracts or immunoprecipitates were separated by SDS-PAGE and immunodetected using the following antibodies: monoclonal against cyclin B1 (GNS1), cyclin A (E72),  $\alpha$ -tubulin (all from Neomarkers); monoclonal anti-hWee1 (Santa Cruz Biotechnology); phosphohistone H3 (Ser10) and hMyt1 (both from Cell Signaling Technology); monoclonal anti-cyclin A E43.2 (kindly gifted by Tim Hunt). Monoclonal anti-poly(ADP-ribose) polymerase (PARP, PharMingen, BD Biosciences, San Diego, CA) was used for simultaneous detection of both PARP and its cleavage product. CDK1 antibodies are described in this section.

### ACKNOWLEDGMENTS

This study was supported by the Belgian Federation against Cancer, the Belgian Fund for Scientific Medical Research (FRSM), the National Fund for Scientific Research (FRS-FNRS, Belgium) and Télévie. H.K. was a fellow of the Fonds pour la Formation à la Recherche dans l'Industrie et l'Agriculture (FRIA) and was also supported by the Fondation Rose et Jean Hoguet and the Fonds David et Alice Van Buuren. K.C. is a FRS-FNRS/Télévie Scientific Research Worker, and P.P.R. is a Senior Research Associate of the FRS-FNRS.

### REFERENCES

Atherton-Fessler S, Liu F, Gabrielli B, Lee MS, Peng CY, Piwnica-Worms H (1994). Cell cycle regulation of the p34cdc2 inhibitory kinases. *Mol Biol Cell* 5, 989–1001.

Bailly E, Doree M, Nurse P, Bornens M (1989). p34cdc2 is located in both nucleus and cytoplasm; part is centrosomally associated at G2/M and enters vesicles at anaphase. *EMBO J* 8, 3985–3995.

Bailly E, Pines J, Hunter T, Bornens M (1992). Cytoplasmic accumulation of cyclin B1 in human cells: association with a detergent-resistant compartment and with the centrosome. *J Cell Sci* 101, 529–545.

Baldin V, Ducommun B (1995). Subcellular localisation of human wee1 kinase is regulated during the cell cycle. *J Cell Sci* 108, 2425–2432.

Baptist M, Lamy F, Gannon J, Hunt T, Dumont JE, Roger PP (1996). Expression and subcellular localization of CDK2 and cdc2 kinases and their common partner cyclin A in thyroid epithelial cells: comparison of cyclic AMP-dependent and -independent cell cycles. *J Cell Physiol* 166, 256–273.

Berthet C, Kaldis P (2006). Cdk2 and Cdk4 cooperatively control the expression of Cdc2. *Cell Div* 1, 10.

Bjellqvist B, Hughes GJ, Pasquali C, Paquet N, Ravier F, Sanchez JC, Frutiger S, Hochstrasser D (1993). The focusing positions of polypeptides in immobilized pH gradients can be predicted from their amino acid sequences. *Electrophoresis* 14, 1023–1031.

Blasina A, Paegle ES, McGowan CH (1997). The role of inhibitory phosphorylation of CDC2 following DNA replication block and radiation-induced damage in human cells. *Mol Biol Cell* 8, 1013–1023.

Bockstaele L, Bisteau X, Paternot S, Roger PP (2009). Differential regulation of cyclin-dependent kinase 4 (CDK4) and CDK6, evidence that CDK4 might not be activated by CDK7, and design of a CDK6 activating mutation. *Mol Cell Biol* 29, 4188–4200.

Bockstaele L, Kookan H, Libert F, Paternot S, Dumont JE, de Launoit Y, Roger PP, Coulonval K (2006). Regulated activating Thr172 phosphorylation of cyclin-dependent kinase 4(CDK4): its relationship with cyclins and CDK “inhibitors.” *Mol Cell Biol* 26, 5070–5085.

Booher RN, Holman PS, Fattaey A (1997). Human Myt1 is a cell cycle-regulated kinase that inhibits Cdc2 but not Cdk2 activity. *J Biol Chem* 272, 22300–22306.

Cheng A, Kaldis P, Solomon MJ (2000). Dephosphorylation of human cyclin-dependent kinases by protein phosphatase type 2C alpha and beta 2 isoforms. *J Biol Chem* 275, 34744–34749.

Choudhary C, Kumar C, Gnad F, Nielsen ML, Rehman M, Walther TC, Olsen JV, Mann M (2009). Lysine acetylation targets protein complexes and co-regulates major cellular functions. *Science* 325, 834–840.

Coulonval K, Bockstaele L, Paternot S, Dumont JE, Roger PP (2003a). The cyclin D3-CDK4-p27kip1 holoenzyme in thyroid epithelial cells: activation by TSH, inhibition by TGFbeta, and phosphorylations of its subunits demonstrated by two-dimensional gel electrophoresis. *Exp Cell Res* 291, 135–149.

Coulonval K, Bockstaele L, Paternot S, Roger PP (2003b). Phosphorylations of cyclin-dependent kinase 2 revisited using two-dimensional gel electrophoresis. *J Biol Chem* 278, 52052–52060.

Darbon JM, Devault A, Taviaux S, Fesquet D, Martinez AM, Galas S, Cavadore JC, Doree M, Blanchard JM (1994). Cloning, expression and subcellular localization of the human homolog of p40MO15 catalytic subunit of cdk-activating kinase. *Oncogene* 9, 3127–3138.

De Boer L, Oakes V, Beamish H, Giles N, Stevens F, Somodevilla-Torres M, Desouza C, Gabrielli B (2008). Cyclin A/cdk2 coordinates centrosomal and nuclear mitotic events. *Oncogene* 27, 4261–4268.

Deibler RW, Kirschner MW (2010). Quantitative reconstitution of mitotic CDK1 activation in somatic cell extracts. *Mol Cell* 37, 753–767.

Ducommun B, Brambilla P, Felix MA, Franza BR Jr, Karsenti E, Draetta G (1991). cdc2 phosphorylation is required for its interaction with cyclin. *EMBO J* 10, 3311–3319.

Fisher RP, Morgan DO (1994). A novel cyclin associates with MO15/CDK7 to form the CDK-activating kinase. *Cell* 78, 713–724.

Fung TK, Ma HT, Poon RY (2007). Specialized roles of the two mitotic cyclins in somatic cells: cyclin A as an activator of M phase-promoting factor. *Mol Biol Cell* 18, 1861–1873.

Furuno N, den EN, Pines J (1999). Human cyclin A is required for mitosis until mid prophase. *J Cell Biol* 147, 295–306.

Gavet O, Pines J (2010a). Activation of cyclin B1-Cdk1 synchronizes events in the nucleus and the cytoplasm at mitosis. *J Cell Biol* 189, 247–259.

Gavet O, Pines J (2010b). Progressive activation of CyclinB1-Cdk1 coordinates entry to mitosis. *Dev Cell* 18, 533–543.

Georgatos SD, Blobel G (1987). Lamin B constitutes an intermediate filament attachment site at the nuclear envelope. *J Cell Biol* 105, 117–125.

Gianazza E (1995). Isoelectric focusing as a tool for the investigation of post-translational processing and chemical modifications of proteins. *J Chromatogr A* 705, 67–87.

Gong D, Ferrell JE Jr (2010). The roles of cyclin A2, B1, and B2 in early and late mitotic events. *Mol Biol Cell* 21, 3149–3161.

Gong D, Pomeroy JR, Myers JW, Gustavsson C, Jones JT, Hahn AT, Meyer T, Ferrell JE Jr (2007). Cyclin A2 regulates nuclear-envelope breakdown and the nuclear accumulation of cyclin B1. *Curr Biol* 17, 85–91.

- Guadagno TM, Newport JW (1996). Cdk2 kinase is required for entry into mitosis as a positive regulator of Cdc2-cyclin B kinase activity. *Cell* 84, 73–82.
- Hagting A, Jackman M, Simpson K, Pines J (1999). Translocation of cyclin B1 to the nucleus at prophase requires a phosphorylation-dependent nuclear import signal. *Curr Biol* 9, 680–689.
- Hagting A, Karlsson C, Clute P, Jackman M, Pines J (1998). MPF localization is controlled by nuclear export. *EMBO J* 17, 4127–4138.
- Heald R, McLoughlin M, McKeon F (1993). Human wee1 maintains mitotic timing by protecting the nucleus from cytoplasmically activated Cdc2 kinase. *Cell* 74, 463–474.
- Hochegger H, Dejsuphong D, Sonoda E, Saberi A, Rajendra E, Kirk J, Hunt T, Takeda S (2007). An essential role for Cdk1 in S phase control is revealed via chemical genetics in vertebrate cells. *J Cell Biol* 178, 257–268.
- Jackman M, Firth M, Pines J (1995). Human cyclins B1 and B2 are localized to strikingly different structures: B1 to microtubules, B2 primarily to the Golgi apparatus. *EMBO J* 14, 1646–1654.
- Jackman M, Lindon C, Nigg EA, Pines J (2003). Active cyclin B1-Cdk1 first appears on centrosomes in prophase. *Nat Cell Biol* 5, 143–148.
- Jin P, Hardy S, Morgan DO (1998). Nuclear localization of cyclin B1 controls mitotic entry after DNA damage. *J Cell Biol* 141, 875–885.
- Katayama K, Fujita N, Tsuruo T (2005). Akt/protein kinase B-dependent phosphorylation and inactivation of WEE1Hu promote cell cycle progression at G2/M transition. *Mol Cell Biol* 25, 5725–5737.
- Katsuno Y, Suzuki A, Sugimura K, Okumura K, Zineldeen DH, Shimada M, Niida H, Mizuno T, Hanaoka F, Nakanishi M (2009). Cyclin A-Cdk1 regulates the origin firing program in mammalian cells. *Proc Natl Acad Sci USA* 106, 3184–3189.
- Kornbluth S, Sebastian B, Hunter T, Newport J (1994). Membrane localization of the kinase which phosphorylates p34cdc2 on threonine 14. *Mol Biol Cell* 5, 273–282.
- Kramer A, Mailand N, Lukas C, Syljuasen RG, Wilkinson CJ, Nigg EA, Bartek J, Lukas J (2004). Centrosome-associated Chk1 prevents premature activation of cyclin-B-Cdk1 kinase. *Nat Cell Biol* 6, 884–891.
- Krek W, Nigg EA (1991a). Differential phosphorylation of vertebrate p34cdc2 kinase at the G1/S and G2/M transitions of the cell cycle: identification of major phosphorylation sites. *EMBO J* 10, 305–316.
- Krek W, Nigg EA (1991b). Mutations of p34cdc2 phosphorylation sites induce premature mitotic events in HeLa cells: evidence for a double block to p34cdc2 kinase activation in vertebrates. *EMBO J* 10, 3331–3341.
- Krek W, Nigg EA (1992). Cell cycle regulation of vertebrate p34cdc2 activity: identification of Thr161 as an essential *in vivo* phosphorylation site. *New Biol* 4, 323–329.
- Larochelle S, Merrick KA, Terret ME, Wohlbold L, Barboza NM, Zhang C, Shokat KM, Jallepalli PV, Fisher RP (2007). Requirements for Cdk7 in the assembly of Cdk1/cyclin B and activation of Cdk2 revealed by chemical genetics in human cells. *Mol Cell* 25, 839–850.
- Li C, Andrade M, Dunbrack R, Enders GH (2010). A bifunctional regulatory element in human somatic Wee1 mediates cyclin A/Cdk2 binding and Crm1-dependent nuclear export. *Mol Cell Biol* 30, 116–130.
- Lindqvist A, Rodriguez-Bravo V, Medema RH (2009). The decision to enter mitosis: feedback and redundancy in the mitotic entry network. *J Cell Biol* 185, 193–202.
- Liu F, Rothblum-Oviatt C, Ryan CE, Piwnica-Worms H (1999). Overproduction of human Myt1 kinase induces a G2 cell cycle delay by interfering with the intracellular trafficking of Cdc2-cyclin B1 complexes. *Mol Cell Biol* 19, 5113–5123.
- Liu F, Stanton JJ, Wu Z, Piwnica-Worms H (1997). The human Myt1 kinase preferentially phosphorylates Cdc2 on threonine 14 and localizes to the endoplasmic reticulum and Golgi complex. *Mol Cell Biol* 17, 571–583.
- Mailand N, Podtelejnikov AV, Groth A, Mann M, Bartek J, Lukas J (2002). Regulation of G(2)/M events by Cdc25A through phosphorylation-dependent modulation of its stability. *EMBO J* 21, 5911–5920.
- Meijer L, Azzi L, Wang JY (1991). Cyclin B targets p34cdc2 for tyrosine phosphorylation. *EMBO J* 10, 1545–1554.
- Merrick KA, Larochelle S, Zhang C, Allen JJ, Shokat KM, Fisher RP (2008). Distinct activation pathways confer cyclin-binding specificity on Cdk1 and Cdk2 in human cells. *Mol Cell* 32, 662–672.
- Moore JD, Yang J, Truant R, Kornbluth S (1999). Nuclear import of Cdk/cyclin complexes: identification of distinct mechanisms for import of Cdk2/cyclin E and Cdc2/cyclin B1. *J Cell Biol* 144, 213–224.
- Nakajima H, Yonemura S, Murata M, Nakamura N, Piwnica-Worms H, Nishida E (2008). Myt1 protein kinase is essential for Golgi and ER assembly during mitotic exit. *J Cell Biol* 181, 89–103.
- Nigg EA (2001). Mitotic kinases as regulators of cell division and its checkpoints. *Nat Rev Mol Cell Biol* 2, 21–32.
- Nilsson I, Hoffmann I (2000). Cell cycle regulation by the Cdc25 phosphatase family. *Prog Cell Cycle Res* 4, 107–114.
- Norbury C, Blow J, Nurse P (1991). Regulatory phosphorylation of the p34cdc2 protein-kinase in vertebrates. *EMBO J* 10, 3321–3329.
- Parker LL, Atherton-Fessler S, Lee MS, Ogg S, Falk JL, Swenson KI, Piwnica-Worms H (1991). Cyclin promotes the tyrosine phosphorylation of p34cdc2 in a wee1 + dependent manner. *EMBO J* 10, 1255–1263.
- Parker LL, Piwnica-Worms H (1992). Inactivation of the p34cdc2-cyclin B complex by the human WEE1 tyrosine kinase. *Science* 257, 1955–1957.
- Parker LL, Sylvestre PJ, Byrnes MJ, III, Liu F, Piwnica-Worms H (1995). Identification of a 95-kDa WEE1-like tyrosine kinase in HeLa cells. *Proc Natl Acad Sci USA* 92, 9638–9642.
- Pines J, Hunter T (1991). Human cyclins A and B1 are differentially located in the cell and undergo cell cycle-dependent nuclear transport. *J Cell Biol* 115, 1–17.
- Pomerening JR, Sontag ED, Ferrell JE Jr (2003). Building a cell cycle oscillator: hysteresis and bistability in the activation of Cdc2. *Nat Cell Biol* 5, 346–351.
- Pomerening JR, Ubersax JA, Ferrell JE Jr (2008). Rapid cycling and precocious termination of G1 phase in cells expressing CDK1A<sup>F</sup>. *Mol Biol Cell* 19, 3426–3441.
- Poon RY, Hunter T (1995). Dephosphorylation of Cdk2 Thr160 by the cyclin-dependent kinase-interacting phosphatase KAP in the absence of cyclin. *Science* 270, 90–93.
- Potapova TA, Daum JR, Byrd KS, Gorbisky GJ (2009). Fine tuning the cell cycle: activation of the Cdk1 inhibitory phosphorylation pathway during mitotic exit. *Mol Biol Cell* 20, 1737–1748.
- Ruiz EJ, Vilar M, Nebreda AR (2010). A two-step inactivation mechanism of myt1 ensures cdk1/cyclin b activation and meiosis i entry. *Curr Biol* 20, 717–723.
- Sanchez V, McElroy AK, Spector DH (2003). Mechanisms governing maintenance of Cdk1/cyclin B1 kinase activity in cells infected with human cytomegalovirus. *J Virol* 77, 13214–13224.
- Santamaria D, Barriere C, Cerqueira A, Hunt S, Tardy C, Newton K, Caceres JF, Dubus P, Malumbres M, Barbacid M (2007). Cdk1 is sufficient to drive the mammalian cell cycle. *Nature* 448, 811–815.
- Schmitt E, Boutros R, Froment C, Monsarrat B, Ducommun B, Dozier C (2006). CHK1 phosphorylates CDC25B during the cell cycle in the absence of DNA damage. *J Cell Sci* 119, 4269–4275.
- Sillero A, Ribeiro JM (1989). Isoelectric points of proteins: theoretical determination. *Anal Biochem* 179, 319–325.
- Solomon MJ (1994). The function(s) of CAK, the p34cdc2-activating kinase. *Trends Biochem Sci* 19, 496–500.
- Solomon MJ, Glotzer M, Lee TH, Philippe M, Kirschner MW (1990). Cyclin activation of p34cdc2. *Cell* 63, 1013–1024.
- Solomon MJ, Lee T, Kirschner MW (1992). Role of phosphorylation in p34cdc2 activation: identification of an activating kinase. *Mol Biol Cell* 3, 13–27.
- Sorensen CS, Syljuasen RG, Falck J, Schroeder T, Ronnstrand L, Khanna KK, Zhou BB, Bartek J, Lukas J (2003). Chk1 regulates the S phase checkpoint by coupling the physiological turnover and ionizing radiation-induced accelerated proteolysis of Cdc25A. *Cancer Cell* 3, 247–258.
- Staufenbiel M, Deppert W (1982). Intermediate filament systems are collapsed onto the nuclear surface after isolation of nuclei from tissue culture cells. *Exp Cell Res* 138, 207–214.
- Szepesi A, Gelfand EW, Lucas JJ (1994). Association of proliferating cell nuclear antigen with cyclin-dependent kinases and cyclins in normal and transformed human T lymphocytes. *Blood* 84, 3413–3421.
- Tassan JP, Schultz SJ, Bartek J, Nigg EA (1994). Cell cycle analysis of the activity, subcellular localization, and subunit composition of human CAK (CDK-activating kinase). *J Cell Biol* 127, 467–478.
- Watanabe N, Broome M, Hunter T (1995). Regulation of the human WEE1Hu Cdk tyrosine 15-kinase during the cell cycle. *EMBO J* 14, 1878–1891.
- Wells NJ, Watanabe N, Tokusumi T, Jiang W, Verdecia MA, Hunter T (1999). The C-terminal domain of the Cdc2 inhibitory kinase Myt1 interacts with Cdc2 complex and is required for inhibition of G(2)/M progression. *J Cell Sci* 112, 3361–3371.
- Yang J, Bardes ES, Moore JD, Brennan J, Powers MA, Kornbluth S (1998). Control of cyclin B1 localization through regulated binding of the nuclear export factor CRM1. *Genes Dev* 12, 2131–2143.
- Yoshida M, Nishikawa M, Nishi K, Abe K, Horinouchi S, Beppu T (1990). Effects of leptomycin B on the cell cycle of fibroblasts and fission yeast cells. *Exp Cell Res* 187, 150–156.